FOI-R--0936--SE
September 2003
ISSN 1650-1942
Scientific report

Björn Montgomerie & Jan-Åke Dahlberg

VORTEX SYSTEM STUDIES ON SMALL WIND TURBINES

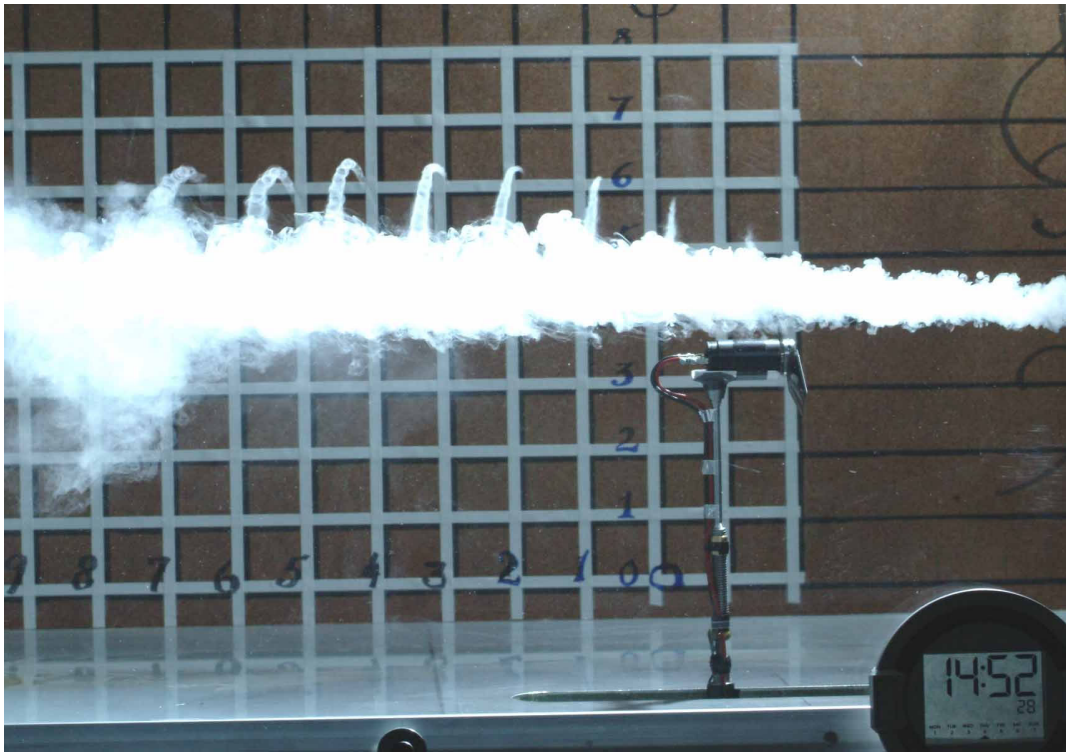

Aeronautics Division, FFA
SE-172 90 Stockholm

SWEDISH DEFENCE RESEARCH AGENCY
Aeronautics Division, FFA
SE-172 90 Stockholm

FOI-R--0936--SE
September 2003
ISSN 1650-1942
Scientific report

Björn Montgomerie & Jan-Åke Dahlberg

Vortex System Studies on Small Wind Turbines

Issuing organization	Report number, ISRN	Report type
FOI – Swedish Defence Research Agency	FOI-R--0936--SE	Scientific report
	Research area code	
	Civil applications	
	Month year	**Project no.**
	September 2003	B827356
	Customers code	
	5 Contracted research	
	Sub area code	
	91 Civil Applications	

Author/s (editor/s)	Project manager
Jan-Åke Dahlberg Björn Montgomerie	Björn Montgomerie
	Approved by
	Sven-Erik Thor
	Sponsoring agency
	Swedish Energy Agency
	Scientifically and technically responsible
	Björn Montgomerie & Jan-Åke Dahlberg

Report title

Vortex System Studies on a Small Wind Turbine

Abstract

The wind tunnel experiment reported included a small wind turbine setup and smoke to visualize the trailing tip vortices for different wind turbine configurations. Several combinations of tunnel wind speeds and tip speed ratios generated a database where the end result functions were radius and pitch, of the tip vortex spirals, versus the downstream coordinate. The Reynolds number in the experiment was very low compared to that of full size turbines. The results should therefore be seen as valid only for low Reynolds numbers. The models were 18 and 25 cm diameter turbines. This is thought to be complementary to the information obtained in similar wind tunnel investigations for much larger models.

The database is meant to be a fundamental tool for the construction of practical aerodynamic induction methods. Such methods typically employ the Biot-Savart law. Howerver, the pure application of the Biot-Savart law has been shown to lead to a flow field, which deviates considerably from that of reality. E.g. the concentration into tip vortices does not happen when the flow is simulated with Biot-Savart law only. Thus, a combination of the induction method and its modification, based on investigations such as the one reported, is foreseen to replace the widely used Blade Element Momentum method for wind turbine loads and performance prediction.

Keywords

Wind turbine, aerodynamics, induction, performance, tip vortex, tip vortices, Reynolds number

Further bibliographic information	Language English
ISSN 1650-1942	**Pages** 27
	Price acc. to pricelist

Utgivare	Rapportnummer, ISRN	Klassificering
Totalförsvarets Forskningsinstitut - FOI	FOI-R----SE	Vetenskaplig rapport
	Forskningsområde 9 Övriga civila tillämpningar	
	Månad, år September 2003	**Projektnummer** B827356
	Verksamhetsgren 5 Uppdragsfinansierad verksamhet	
	Delområde 91 Övriga civila tillämpningar	

Författare/redaktör	Projektledare
Björn Montgomerie Jan-Åke Dahlberg	Björn Montgomerie
	Godkänd av Sven-Erik Thor
	Uppdragsgivare/kundbeteckning Energimyndigheten
	Tekniskt och/eller vetenskapligt ansvarig Björn Montgomerie & Jan-Åke Dahlberg

Rapportens titel (i översättning)

Studier av rotorspetsvirvlar hos små vindturbiner

Sammanfattning

I ett vindtunnelexperiment har turbinbladens spetsvirvlar studerats med hjälp av injicerad rök. Med kamerans hjälp dokumenterades virvlarna för olika kombinationer av konfigurationer och andra förutsättningar. Genom avläsning av fotografierna kunde virvelkärnornas centrum fastställas inom varje fotografi. Genom att ta 9 redundanta bilder fastställdes ett medelbeteende som i nästa steg fångades i några enkla kurvanpassningsformler (polynom). Dessa beskriver spetsvirvlarnas spiralform som radie och stigning, båda som funktion av koordinaten i strömningsriktningen. Genom att använda sig av polynom kunde hela experimentets alla radier och stigningar beskrivas i en databas med siffersatta värden på polynomkoefficienterna.

Reynolds tal var mycket lågt i jämförelse med fullstorlek. Resultaten gäller därför endast för små Reynoldska tal. Modellerna var 18 och 25 cm i diameter. Tanken var att detta skall vara kompletterande information till data från större modeller med motsvarande mätningar. Detta kan användas till att ge flera punkter på en kurva med storleken på x-axeln. Vidare kommer databasen till användning då moderna induktionsmetoder skall konstrueras och ersätta de gängse bladelement-impuls-metoderna. Rena induktionsmetoder har visat sig ge resultat som inte överensstämmer väl med verkligheten. En framtida kombination av induktionsteori och observerade resultat från mätningarna bedöms vara en stor förbättring jämfört med dagens metodik för beräkning av laster och prestanda.

Nyckelord

Vindturbin, aerodynamik, induktion, prestanda, spetsvirvel, spetsvirvlar, Reynolds tal

Övriga bibliografiska uppgifter	Språk Engelska
ISSN 1650-1942	**Antal sidor:** 27
Distribution enligt missiv	**Pris: Enligt prislista**

Acknowledgements

This study was supported by the Swedish Energy Agency.

All interpretation and compilation to geometric description of the vortex spirals, based on the many photographs from the wind tunnel, was carried out by Karin Åhlund, engineering student at Mälardalens Högskola in Västerås, Sweden.

CONTENTS

NOTATION

A, B, C, D, E and F = coefficients in the curve fit equations, see Appendix A.
A, B and C = Notations for three rotor configurations.
E.g. A88 = Rotor A and pitch for the two blades is 8 deg.
E.g. A610 = Rotor A with different pitch for the blades, i.e. 6 and 10 degrees
BEM = Blade Element Momentum
BEI = Blade Element Induction
Cp = Power coefficient
CT = Thrust coefficient
Pitch means two entirely different things. One meaning is the blade pitch angle. The other meaning is the distance between adjacent tip vortices. The latter pitch must be multiplied by 2 in order to get the pitch of one tip vortex spiral. The reason is that the reported pitch is the downstream distance between one vortex and the next. The two are vortices intertwined from two blade tips like threads on a double-threaded screw. Therefore they are at about half the pitch of one spiral.
p_v = Tip vortex pitch (= distance between consecutive vortices, m)
R = Turbine tip radius
r_v = Tip vortex radius (m)
TSR = Tip Speed Ratio
V = Speed = Wind tunnel wind speed, m/s
X = The downstream coordinate, which is zero at the rotor disk (m)
$x = X/R$

VORTEX SYSTEM STUDIES ON SMALL WIND TURBINES

Björn Montgomerie - Jan-Åke Dahlberg
Swedish Defense Research Agency (FOI), Aeronautics Div., (FFA)
September 2003

1.Introduction

An experiment, that this report describes, was set up to derive data in support of horizontal axis wind turbine performance prediction. Techniques used to predict horizontal axis wind turbine performance may employ trailing concentrated vortices and induction calculation. The Biot-Savart law for induction is used to calculate the induced velocity vector anywhere in three-dimensional space. This includes the possibility to evaluate the velocity vector on selected blade elements. Then the calculation of aerodynamic forces on the blades is a straightforward matter leading to loads and performance assessment. It is proposed to call the described method the Blade Element Induction method (BEI). This technique eliminates the need to iterate the induction by a search for a balance between the thrust on the rotor and the momentum flux lost in the wake. The latter method, called the Blade Element Momentum method (BEM), is still generally used today. It is known, however, that the pure induction methods will lead to a vortex pattern, which is quite different from that of reality. The purpose of this test was to extract data showing the true paths of the trailing tip vorticity for different configurations, wind speed and tip speed ratios.

2.Wind Tunnel and Turbines

The centerpiece of the test is a small two-bladed turbine whose blades are replaceable. This arrangement is visible in Fig. 1. The pitch setting of the blades is arbitrary since the blade shanks have circular cross section fixable to the hub sockets. A few sets of blades were available. Besides another unpitchable rotor (see Fig. 6) was tested.

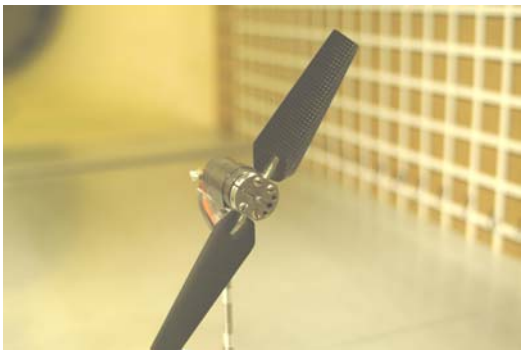

Figure 1

The turbine was placed in a wind tunnel denoted LT5. The overall tunnel arrangement is seen in Fig. 2.

Appearing from left to right is the centrifugal fan (black), which expels the tunnel flow through an open window (also visible). The yellowish soft-shaped object is the square-to-circular fiber glass and plastic

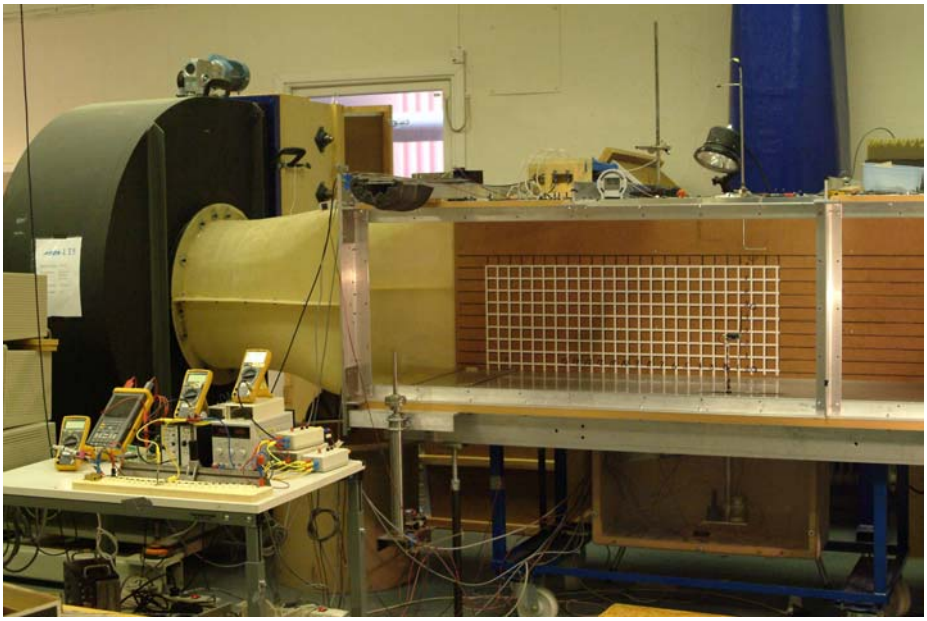

Figure 2

adapter, which conducts the air from the test section to the fan.

There is a visible coordinate system on the inner side of the visible wall along the test section. That system can be viewed through the front wall, which is made of a transparent acrylic material. The turbine discretely covers the right lower part of the coordinate system.

Outside of the transparent wall (on the hither side of the tunnel in Fig. 2) there is a digital camera for the recording of the turbine, the smoke and the coordinate system. That camera is not visible in the picture since it was used to take the picture. The air enters through an opening to the right outside of the picture. The opening is furnished with rounded lips to form an intake with minimized peripheral turbulence. The intake cross section is covered by a grid, which helps even out any incoming turbulence. The turbulence is further reduced by a modest contraction of the flow cross sectional area from the intake to the test section. The intake is located going through a wall to an adjacent large hall, whose large cargo transportation doors to the outer world are held wide open during testing. Since both the entrance and exit of the air flow are connected with the air outside the building, the tunnel is somewhat sensitive to external meteorological conditions. This prevents operation when it is significantly windy.

The length of the test section is 2.5 m with a cross-section of 0.9x 0.675 m and a velocity range of 5-16 m/s. The wind tunnel was originally designed and built as a low-cost tunnel intended for anemometer development and calibrations. Due to a low contraction ratio the turbulence intensity is rather high, 0.3%, and the flow in the tunnel is somewhat inhomogeneous with spatial variations. The wind speed at the position of the test object is measured using a pitot tube mounted in the ceiling of the test section, as seen in Fig. 2, where it, and its shadow, appear as the letter “L” above the coordinate system.

A hole in the tunnel wall was used to insert a smoke generator.

3.Turbine blades

3.1 Pitchable Rotor

The 180 mm diameter turbine (basic rotor/turbine A) consists of two non-twisted blades, see Fig. 1 and 3, with Göttingen 417A airfoils, see sketch at the top of Fig. 12. This thin airfoil was selected because of its supposedly good performance at low Re-numbers. As it would turn out the performance was at best mediocre. The blades were made of reinforced epoxy. Four layers of carbon fiber fabric gave a thickness of about 0.5 mm. The blades are tapered such that the tip chord is 16 mm and the maximum chord at 12% radius is 27 mm. This gives a solidity (blade area/swept area) of 13%. Each blade is attached to the 23 mm diameter hub by means of a 3 mm diameter screw glued to the blade parallel to the 25% chord line. The blades can be set to any pitch angle as explained below. Another set of blades, not depicted, with clipped leading and trailing edges, had lesser chord. This is referred to as “rotor/turbine B”. Its tip chord and biggest chord respectively were 10 and 19.5 mm corresponding to a solidity of 9%. The big chord was located at 12% radius. Pitch for both types was defined as the pitch of a tangent from the pressure side leading edge to the trailing edge at 85% of tip radius.

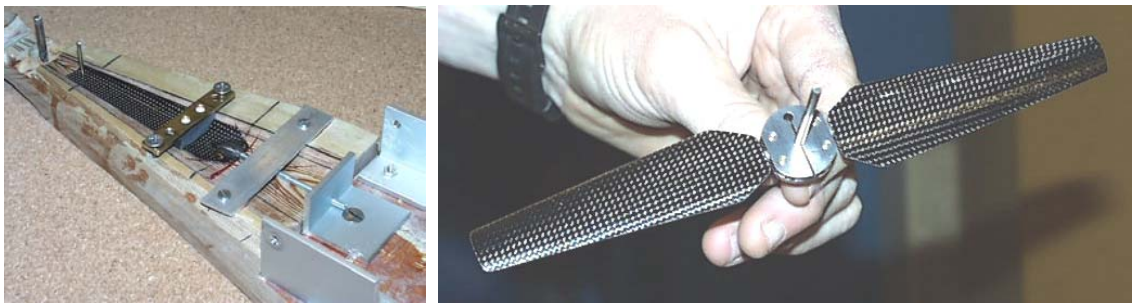

Figure 3 - The blade placed in the mould for attachment of the pitch axis (left). A complete rotor with two blades mounted to the hub (right).

3.2 Blade Pitch Setting

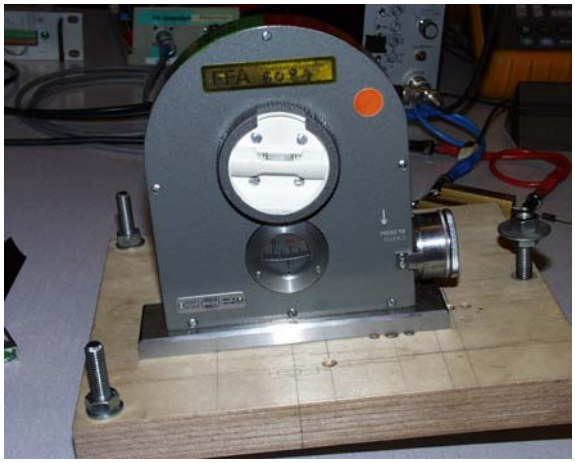

Figure 4 - Inclinometer

Figure 5 - Level

The setting of the pitch angle, for rotors A and B, was made in a dedicated set-up, which enables the pitch of each individual blade to be set. The detached rotor was placed on an adjustable board with the pressure side of the blades up, using a very sensitive water level placed across the chord as seen in Fig. 5. On the same board an inclinometer was used to measure the board uptilt, see Fig. 4. The level thus rested on the leading and trailing edges of the thin sheet airfoil. By raising or lowering the board angle a measurable number of degrees, using the inclinometer, and adjusting the blade pitch until the blade chord became horizontal the blade pitch could be determined with an accuracy better than 0.1º.

3.3 Fix Pitch Rotor

Figure 6
Fixed pitch rotor turbine C

A larger non-pitchable rotor, which is attachable to the same shaft and generator, has a tip to tip measure of 246 mm. It has twist, camber and formed profiles with rounded leading edges and sharp trailing edges. Its solidity is 14%. Because of the geometry this rotor gave a higher maximum power coefficient than both of the A and B rotors.

The characteristic geometric measures consist of distributions of cross section profiles, chord length and twist. The rotor was produced by casting. Several identical rotors were cast in the same mold. One rotor was cut up in pieces to allow photographing the sections. The pictures of the sections and the global geometric characteristics of the rotor are found in App. B.

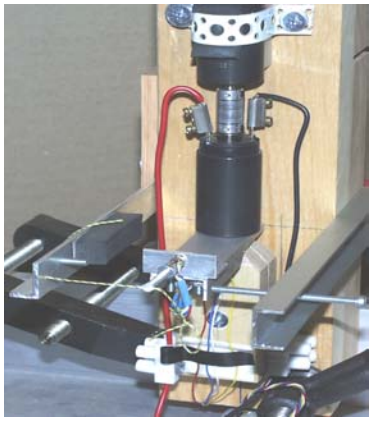

Figure 7 -The set-up for calibration of generators

4. Generator Calibration and Load Circuit

4.1 Calibration

The hub is directly attached to the 3 mm diameter shaft of the generator, which is a 24V DC motor. The motor has permanent magnets and is used as a generator. This type of generator is suitable since it has a straight torque vs current relationship, which is determined through calibration. The set-up for calibration

is shown in Fig. 7 . The upper motor is driving the shaft to the lower generator. The house of the generator has a limited freedom to rotate. When the generator is loaded, the reaction torque is absorbed by an arm equipped with strain gages.The RPM of the upper motor is controlled from the computer and the lower generator to be calibrated is loaded with resistors. Rotational speed, current and torque are recorded.

A typical result from the calibration is seen in Fig. 8. The offset, in the linear curve fit, is caused by friction

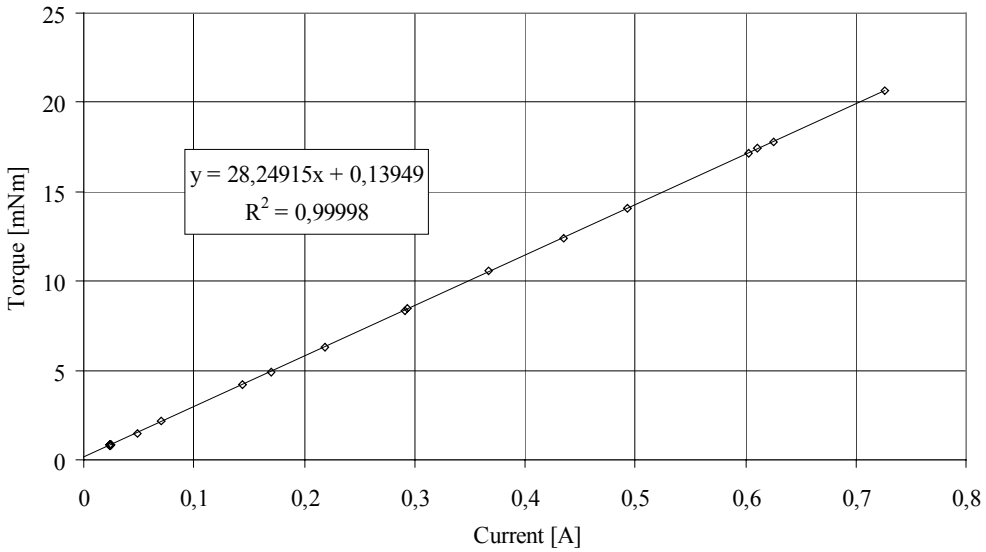

Figure 8
A typical result from calibration of a generator with a straight line fit through the measured points

in brushes and bearings. Therefore a corresponding free spin small aerodynamic power exists.

4.2 Load Circuit

In the test runs the turbine generator poles were connected over one resistor, with known resistance, and a selectable number of diodes. The electrically sensitive points between the diodes were given order numbers from 0 to 23. These points were manually accessible by attaching a connector, thereby controlling how many diodes that participated in the circuit. As the generator RPM is initially increased the voltage increases over the circuit without any significant current, other than a very small leakage, going through the diodes. As soon as the voltage over each diode exceeds a certain saturation level the diode yields and lets the current through. The generator very quickly finds its balance between the driving external aerodynamic rotor torque and the braking generator torque and the RPM becomes steady. This arrangement provides one RPM for each connector point, although any value of the RPM cannot be freely chosen.

5. Smoke Generator

A smoke generator was created during the course of the project. It uses propanediol ($C_3H_8O_2$), which is pumped into a heat chamber and electrically heated. The heat chamber is located inside a metal pipe. The pipe is housed in a boom with some heat protection to the outside. The internal diameter at the end of the pipe (the nozzle) is reduced to provide a moderate pressure in the heat chamber. The pump flow and the heating power are adjustable. The pump and the container of the liquid constituted one relatively heavy unit to occupy a fixed position during testing. The much lighter boom was connected, by a flexible tube and electric wires, to the fixed unit. This arrangement allowed the fluid to be transported from the fixed unit to the boom and the boom to be manually moved during testing to inject the smoke at any desired point in the tunnel. The tunnel wall had a hole in the side through which the smoke generator could be moved freely by hand and fixed when a good position was established. When operated the arrangement provides a white smoke coming out of the nozzle.

6. Turbine Performance

The power was calculated from RPM, voltage and the known resistance over the resistor. The current was calculated from the voltage and the resistor resistance. Then the equation in the diagram in Fig. 8 was used

to get torque. The turbine power may then be obtained through multiplication by the rotational speed. The thrust came from the thrust sensor, see the data acquisition section. Power and thrust, and the corresponding coefficients, constitute the *performance* of the turbine in the vocabulary used in this report.

The performance was measured in the wind tunnel by having constant wind speed and manually loading the turbine by using a different number of diodes in the diode/resistor circuit. For each load case wind speed, RPM, torque and thrust were recorded during 10 seconds and an average was calculated on-line. Practically all connection points on the board of diodes, except for 5 m/s, were used to give a dense distribution of RPM values. After post processor data reduction, the performance, in terms of power coefficient C_P and thrust coefficient C_T, versus tip speed ratio TSR, could immediately be plotted for inspection. A summary of the performance for basic rotor A is seen in Fig. 11.

7. Using Smoke

The blade tips emit concentrated vortices, as do airplane wings in flight. Since the turbine rotor rotates, while giving off tip vortices, the vortices become helical. Also the roots of the blades generate trailing vorticity. In order to identify the vortices they were made visible by means of injection of smoke upstream of the turbine. If the smoke is injected at a strategically chosen point the individual tip vortices become clearly visible as holes or spiral shaped "ribs" (like ribs on a rib cage of a skeleton). It is believed that the mass of the droplets in the smoke is subjected to centrifugal forces, which thins down the vortex core contents of smoke. It therefore appears dark. The root vorticity does not lend itself to easy portrayal because the vorticity is not concentrated except for a tiny area in the immediate vicinity of the blade root. Therefore, no photographic recordings could be analyzed for root vortex travel identification.

Examples of the two types of tip vortex visualizations are seen in the figures below. The rib shape, Fig. 10, is explained by the fact that, inside the vortex core, there is a longitudinal flow following the spiral, as well as a rigid body rotation. The smoke is trapped in this stream and thins down farther away from the major smoke supply and truncates the view of the vortex cores. If the thinning of the rib smoke occurred more slowly the full spirals would have been visible. It is the truncation that gives rise to the illusion of "ribs".

The photographs are the only source of information for the tip vortex geometry. Thus the photographs need to be read off by the human eye and the coordinates must be established as described in the next section.

Figure 9 – Smoke injected to hit top of turbine disk

Figure 10 – Smoke injected to hit turbine disk at 10 o'clock

8. Identification of the Tip Vortex Trails

From the two possibilities of capturing the location of the tip vortices the one corresponding to Fig. 9 (the core view) was chosen. There are arguments in favor and against for both types as far as it concerns finding the radius and pitch of the tip trails. For some tip speed ratios the ribs are not so apparent, while the core view reveals more of the vortex makeup. The center of the dark spots in the vortex was assumed to be representative of the location of the vortex. The reduction of the photographic material into xyz information was accomplished as described in Sect. 9. The complete test matrix is seen below.

Table 1 – Test matrix summary

Wind speed	Pitch = 6° Rotor A	Pitch = 7° Rotor B	Pitch = 8° Rotor A	Pitch = 10° Rotor A	Pitch = 6/10° Rr A	Fix pitch Rotor C
5	45	-	45	45	0	45
6	-	-	-	-	-	36
8	45	45	45	45	45	36
12	45	-	45	45	0	0

The following information makes it possible to interpret the table. – The removable blades, as depicted in e.g. Fig. 1, were trimmed to pitch the two blades equally, see columns 2, 3, 4 and 5. As a matter of interest, for a faulty pitch system, the two blades were pitched differently (6° and 10°) as seen in column 6 of the table.

The number 45 is frequently present in the matrix. It signifies the number of photographs that was taken during the testing. This number arose from having 5 different resistor settings (results in 5 different tip speed ratios) and taking 9 photographs for each V/pitch/diode combination. The number of diode settings (= number of tip speed ratios) can be calculated from the number in the table if divided by 9. As it would turn out, almost all photographs were good enough "to make it" through the screening process before being used. The few that were excluded were pictures taken at the lowest TSR values where induction calculation is not very sensitive to assumptions about the traveling geometry of the tip vortices.

9.Data Acquisition

9.1 Overview

The set of signals that was monitored during the testing follows.

Voltage representing RPM
Pressure representing Wind speed
Voltage representing Thrust
Voltage over the resistor in the RPM control circuit
Ambient pressure (manual)
Tunnel air temperature (manual)

A laser pen was located on top of the tunnel. RPM was measured by letting the laser beam go through the transparent top of the tunnel, through the rotor disk and ending at a photo diode on the floor of the tunnel. A blade passage generated a pulse from the sensor circuit to the computer. After sampling, division by two (for two blades) and average formation the RPM was established and funneled to the output file along with the other companion signals. As a check a multi-meter readout provided the analyst with direct on-line information of the frequency from the photo diode as well. The corresponding equipment is seen in Fig. 2.

The wind speed was taken from the Prandtl tube in the ceiling of the tunnel at the same station as the turbine disk. Because of the turbine blockage effect this point is representative for the tunnel speed at all levels of blockage. This introduces a speed error less than 1.5% according to pressure mappings done in previous testing sessions. However, the flow surrounding the wake is accelerated.This should have an effect, on the tip vortices, to be accounted for in future use of the database.

The thrust was indirectly measured by means of a moment balance located close to the bottom of the tower. The balance was calibrated by applying known loads in the center of the rotor. This requires the resultant of the forces, acting on the blades, to be located in the center of the rotor. The accuracy was considered to be acceptable for the purpose of this test.

The RPM control circuit consisted of the choice of diodes and a resistor – all in series. The voltage over the resistor, was measured and used to determine the current, which translates to torque using the relationship of Fig. 8. Power is then obtained from multiplication by the rotational speed. The resistor is considered sufficiently insensitive to temperature variations not to need compensation. The ambient pressure was read

off an accurate barometer and the pressure was hand noted on paper for input to the computer post processor program. The tunnel temperature was read and noted in the same way. The temperature sensor was located inside the tunnel and near the tunnel exit after the fan.

Both the pressure and the temperature were used as input to the computer program, to calculate the air density to be used to calculate Cp and C_T.

The photographs, of the type seen in Fig. 9, provide the basis for evaluation of the geometry of the tip vorticity. During all runs the data recording was active, thus providing an accumulation of signals sent to an output file. These files include a clock stamp. In order to match the photographs to the correct performance circumstances a clock was included in each picture. The time of the clock would later be used to match the correct file including the signals listed above. No evaluation of the vortex circulation is possible with this method. Only position can be provided. The tip vortex geometry is intended to be used in the development of empirical methods, which aim at the application of aerodynamic induction theory. Such theories typically use the Biot-Savart equation.

The complete geometrical information is considered to be radius and pitch of the smoke spirals. Both radius and pitch are functions of the downstream distance from the rotor. The simplifying assumption was made that the spirals are polar symmetric. Thus, any information about the radius is good enough, e.g. the vertical radial distance from the turbine shaft centerline to the tip vortex core. To obtain this information the photographs were evaluated primarily by measuring this distance with the aid of a reference coordinate system painted on the wall as seen in Fig. 2. Besides a set of equations was established such that in the analysis the computer screen window coordinates expressed in x pixels and y pixels were fed into these equations and implemented in a spread sheet program. The method in brevity can be described as follows.

The camera was located at close distance from the tunnel. This causes parallax errors if not accounted for. Therefore a stereometric compensation method was developed. The input to this method included the position of camera, turbine, origin and lengths of axes of the painted coordinate system, obliqueness of same system and a few more parameters.

The x and y pixel information was converted into real world coordinates such that the down-stream coordinate was associated with x, the vertical with y and the horizontal across the flow, pointing from the viewer toward the far wall of the tunnel, became the z direction. In fact, this z direction coordinate was an input to the method for the evaluation of the final x and y values, but as it turned out z = 0 was used in all cases. The origin of this system is located in the center of the rotor disk.

Using the photographs and the method together provided the final geometrical data for the tip vortex positions for each photograph. Since 9 photographs were available per case statistical mean curves could be established for radius and pitch as functions of x. Each such case is characterized by wind speed and TSR (for each configuration of the rotor). It may be of interest to notice that the Reynolds number effect, caused by the variation in wind speed, appears with clarity in the performance data, see Fig. 11.

9.2 Obtaining Performance

The acquisition of the performance data included several details in its sequence as follows.

9.2.1 *No Smoke*

1.Case definition and setup:

- a. Select rotor
- b. Adjust blade pitch
- c. Read ambient air pressure
- d. Read tunnel air temperature (fan operating)

2.Measure zero wind speed conditions

- a. Turn off the fan and let settle for 30 seconds
- b. Run computer data acquisition program and record wind speed, RPM etc. This is done so zero drifts and adjustments can be identified and accounted for later.

3. Set RPM using diode connection point – one of 24 positions (see Fig. 2 the wooden board on the table and the text in Sect. 5)

4. Run data acquisition program and record basic engineering quantities such as wind speed, RPM etc. accumulating same type of data for each wind speed. At the same time hand written notes were made. These included the diode point, camera position, data acquisition sampling frequency, number of samples, turbine definition and any information judged to be of interest.

5. If RPM cases remain go to step 3, else continue.

6. Run off-line file conversion program using the file from step 4 as input. Create Cp, CT, TSR etc.

7. Plot Cp and CT versus TSR (= performance information).

9.2.2 *Using Smoke*
At this point the full span of the interesting part of the TSR range was available with points that were rather densely placed on the Cp and CT curves. A reduced selection of TSR points was then made. These points were used to repeat a reduced set of the steps from 2 to 7. During these steps photographs were taken. The reduction of RPM values was suitable and necessary. Several smoke pictures were taken from the same case, as defined after step 3, and since there were 24 resistor settings the number of photographs would be unwieldy to handle if no reduction of points was to be made. Secondly the main interest for tip vortex tracing is from a little below TSR, at maximum Cp, to high TSRs. Therefore small values of TSR can be discarded and a high density of points would not add any essential information to the tip vortex behavior. The described sequence of steps was thus modified such that, in step 4, the data collection is run twice, for redundancy check, with 9 photographs taken in between. In all cases the sampling frequency was 100Hz throughout the testing.

The end result from the described activity is again performance points that can be plotted in the same diagram as was previously produced without smoke. Any obvious deviations would show up immediately. As it turned out there was no significant change of performance, meaning that the data points taken with smoke neatly took place on the previous curves although not quite at identically the same points. Based on this evidence it could be concluded that the smoke injected did not disturb the flow significantly.

9.3 Data from the Photographs
The coordinates of the smoke trails were captured from the centers of the tip vortices as described in Sect. 8. The radius then becomes equal to the y coordinate obtained in mm. The pitch between tip vortices was likewise obtained in mm. After division by the rotor radius both of these measures were made dimensionless. As a next step a 3rd order polynomial curve fit was created to simulate the radius versus downstream coordinate characteristics while the spiral pitch characteristics can be captured using either a constant value or a linear relationship.

For each combination of TSR, wind speed and rotor configuration the essential aerodynamic characteristics could thus be condensed into Cp, CT and a few polynomial coefficients.

General observations, pertinent to the tip vortices, were that the radius keeps increasing far behind the turbine and that the pitch is practically constant, possibly with an increase toward the end.

10. Results

An example summary, of the global performance parameters, is presented in Fig. 11. Wind speeds, in rising order, are seen to cause increasing levels of the Cp curve apex. It is believed that this is a Reynolds number effect on profile drag. For the corresponding CT curves there is hardly any difference. These data were produced without smoke or photographs.

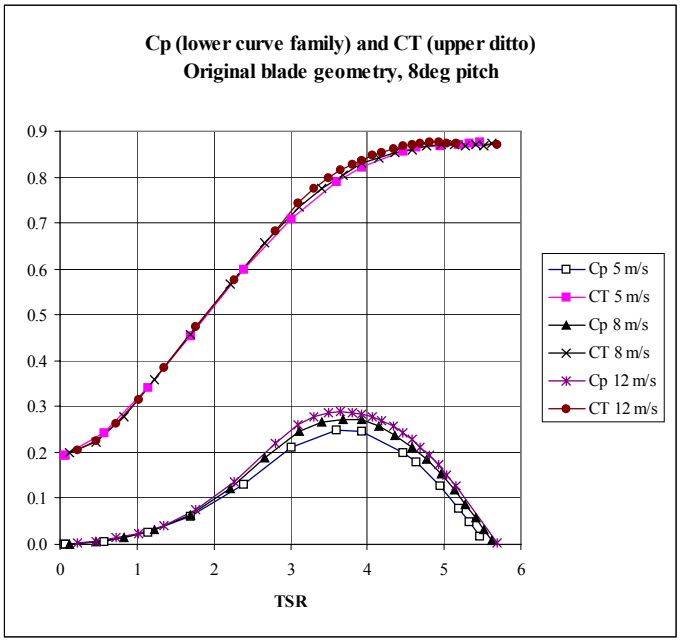

Figure 11 – Rotor A, performance at 8 degrees of pitch for three values of V = 5, 8 and 12 m/s

Later, data points of Cp and CT, collected during the two dedicated data takings, that preceded and followed the photographing part of each *case cycle*, were found to gather on the same curve. Any drift of the signaling equipment, during the cycle, would have been revealed by this technique. During the testing it was seen that all data points appeared on the same curve. The equipment was thus capable to generate data of good repeatability with or without smoke. This conclusion was reinforced by the data taken at no wind before and after a set of tip speed ratios where the pressure sensor signal was found to be equal before and after. Each such major cycle included five RPM cycles with photographs taken. The total drift of the pressure, during such a sequence, was insignificantly small in all cases used in the analysis and almost no data had to be discarded.

For a well designed full size turbine a maximum Cp value of about 0.45 should be expected. This is to be compared with values around 0.28 as seen in Fig. 11 and valid for the A turbine. This turbine has several afflictions, which are detrimental to good performance. The very thin airfoil in combination with a lack of twist together with a very small Reynolds number should be expected to always give rise to massive separation somewhere along the radius. Therefore a high blade profile drag results, although the opposite

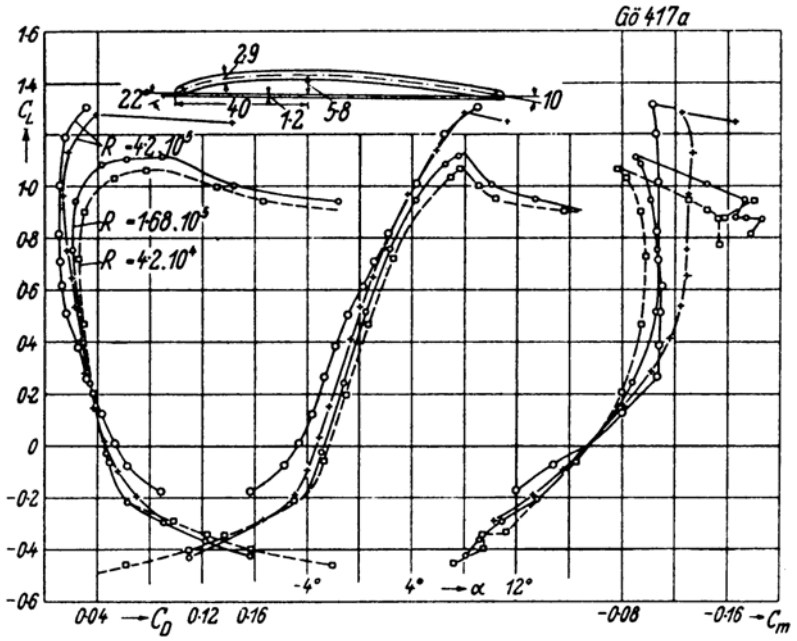

Fig. 12 – Aerodynamic data from Riegels, Ref. 1

was expected based on comparative information of 2D profiles tested in wind tunnels. High profile drag causes poor performance. The aerodynamic characteristics, for the Göttingen profile used on the turbine,

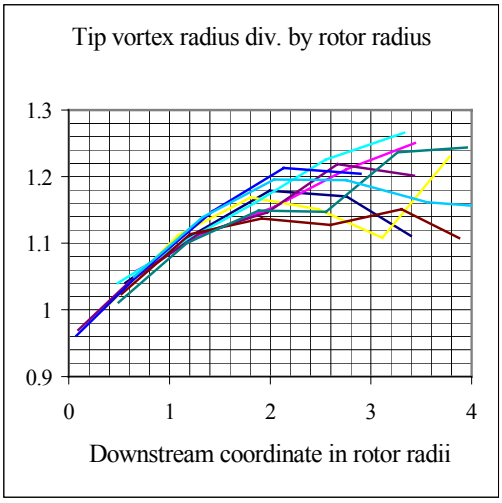

Figure 13

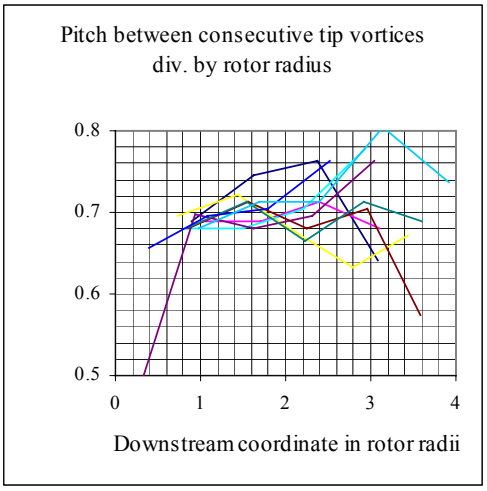

Figure 14

appear in Fig. 12. In the LT5 tunnel speeds of 5, 8 and 12 m/s correspond to Reynolds numbers, based on the tip chord, equal to 21000, 33300 and 50000 respectively. Average curves were formed from the 9 curves. The averaging was carried out using a dedicated Fortran program, which was made to handle several problems as follows.

From each average curve a functional relationship between the downstream coordinate and radius and pitch was established as curve fit polynomials. Thus the batch of photographs per case provides its scientific content in the condensed form of a few polynomial coefficients. One example follows. The configuration is the basic rotor A with blade 1 and blade 2 at the same pitch angle 8 degrees, TSR = 3.5 and Wind speed = 12.3 m/s

It is seen how the characteristics of the vorticity can be represented by two parameters, i.e. radius of tip vortices and the pitch between the spirals from the two blades. If one single spiral is to be characterized by its pitch the ordinate values in Fig. 14 must be doubled. This is because the tip spirals are intertwined from two blade tips.

A polynomial curve fit of the third order was adapted to the vortex radius curves. Such an expression requires 4 constants. A search in four-dimensional space gave rise to the optimum values of A, B, C and D. The search method is available in the Excel program.

$$\frac{r_{Vortex}}{R_{rotor}} = A + Bx + Cx^2 + Dx^3$$

For the particular case discussed here the numerical values were

$A = 0.948207$
$B = 0.175851$
$C = -0.03732$
$D = 0.001796$

Likewise the curve for pitch (between the vortices from the two blade tips) was adapted to a linear fit. For several of the investigated cases the best representation is a constant value. For a relatively large minority of the curves the pitch is constant at first, then it becomes more disorganized and its value increases. In the

database only a linear curve fit is presented for the pitch function. For the particular case chosen for the example the following constant value was found.

$$\frac{pitch}{R_{rotor}} = .78$$

The data quality differs from a mid-position in the x interval to the flanks. Very close to the rotor only one or a few curves exist. That is also the case far downstream as is seen in Fig. 13 and 14.

This observation lead to the construction of a "confidence" function as follows.

$$Confidence = (1 - RMS)\left(1 - \frac{1}{nCurves + 1}\right)$$

First the Fortran program was written to read up the 9 curves, radius or pitch as the case might be. It was also used to do the following.

The Root Mean Square (RMS) value was created from the average of the curves and the curves themselves. For each value of x a different number of curves can be found (except in the mid-range where the number of curves always was = 9. The confidence function therefore tends to drop from about .9 to values approaching zero close and far from the disk. The confidence was used as a weight function when finding the coefficients A, B etc. More specifically a method was developed and implemented as follows.

A straight algebraic average was formed by the program, at x values predetermined in the program. These predetermined points were more densely packed than those of the data points. The predetermined points had generally not the same x values as the data points. Thus interpolation was necessary. The confidence function values were also generated in the Fortran program. The resulting average curve and confidence were saved in an output file, which was directly readable into the spread sheet program Excel. Here e.g. the spiral radius and the confidence appeared as two columns of the same length, both being valid for the same values of x in a third column. A fourth column was created from the curve fit expression. From the average column, the curve fit column and the confidence column an "error" column was created as indicated by the following expression.

$$Error = Confidence \cdot (curveFitRadius - tipVortexRadius)^2$$

Then the error column values were summed and an optimization capability in Excel was used to minimize the error sum by manipulation of the values of the coefficients A, B etc.

The pitch was treated likewise but, as pointed out above, only a linear curve fit was applied.

It is pointed out that some Cp figures are very close to zero, but not quite equal to zero. The cases, for which these circumstances are characteristic correspond to a free spinning rotor. The reason the Cp number, in these cases, is not identically equal to zero is mechanical friction as explained in Sect. 4.1.

It may be noteworthy that the trend of the radius toward the turbine (left in the diagram of Fig. 13) points to a turbine radius of about 95% of the turbine radius. This number appears to be governed by the blade load distribution.

As for accuracy of the results 19 repetitions of the running conditions, at Cp maximum, turned out a RMS value of 0.7%. The absolute error trend is not known. But great effort was put into calibrations of all signals to minimize the absolute error.

11. Conclusions

It can be concluded that:

1.The Reynolds number, in the 20 000 to 50 000 range, has a strong influence on Cp and a weak influence on CT.

2.The variable paths of the tip vortex, observable in e.g. Fig. 13 and 14, do not affect performance noticeably. I.e. power fluctuates very little compared with the apparent vortex radius from one picture to another.

3.Vortex breakdown occurs a little before two diameters downstream of the rotor.

4.Close to the turbine the tip vorticity appears to be coming from a radial position of about 95% in rotor A, 97% in rotor B and 97% in the fix pitch rotor. This is directly readable in the polynomial coefficient A, see App. A. It can be conjectured that the form of the blade loading determines this point. The steeper the decline of loading at the tip the higher the percentage value.

5.The geometry of the tip vortex, in the experiment, is different from what comes out of numerical results using the Biot-Savart law only. The latter typically expands the radius rapidly at the same time reducing the pitch. The observed results increase the radius more continuously and maintains a constant pitch for as long as vortices can be observed before they break up. The analytical methods that will be based on these results must somehow model what is observed and also use some form of induction. The induction technique allows modeling dynamic flow events. Both models must therefore become a necessity in the modeler's calculation tool box.

6. The data obtained are not complete for a calculation of performance. Information about the circulation of the tip vortices is missing. Complementary information is, however, available from Ref. 3 where the same turbine was run in a different wind tunnel with wake flow mapping using hot wire technique.

12. References

1. F. W. Riegels
"AEROFOIL SECTIONS, Results from Wind Tunnel Investigations, Theoretical Foundations"
Translated version from German to English
Butterworth & Co. (Publishers) Ltd. 1961
Originally published under the title "Aerodynamische Profile" by Verlag R. Oldenbourg, Munich 1958

2. XFOIL 6.9 User Guide
Mark Drela, MIT & Astro and Harold Youngren, Aerocraft Inc.
Jan 2001
(The most recent version of the program XFOIL is presently available at http://raphael.mit.edu/xfoil/)

3. Measurements on a wind turbine wake: 3D effects and bluff-body vortex shedding
to be presented at the Delft University in April 2004 by Davide Medici presently doing doctorial thesis work at the Royal Institute of Technology (KTH), Stockholm, Sweden.
Much more data, than those to be presented at the Delft conference, have been retrieved during the wind tunnel testing at KTH. The corresponding database is complementary to the data of this report.

APPENDIX A - **Summary of Results**

In this appendix a summary, of several recorded cases, is presented as polynomial coefficients whose meaning is described in the main report. The coefficients are used to reproduce the wind tunnel results with respect to radius and pitch of the tip vortex spirals.

Notation:

Speed = Tunnel wind speed, m/s; TSR = Tip Speed Ratio
Cp = Power coefficient; CT = Thrust coefficient
r_v = Tip vortex radius (m)
p_v = Tip vortex pitch (= distance between consecutive vortices, m)
R = Turbine tip radius (m)
X = The downstream coordinate, which is zero at the rotor disk (m)
$x = X/R$

$$\frac{r_v}{R} = A + Bx + Cx^2 + Dx^3$$

$$\frac{p_v}{R} = E + Fx$$

	Blade						Tip vortex radius			Tip vortex pitch	
Config	pitch	Speed	TSR	Cp	CT	A	B	C	D	E	F
A1010	10	12.29	4.839	0.187	0.799	0.954194	0.173914	-0.02035	-0.00213	0.82939	-0.01006
		12.24	2.628	0.208	0.619	0.96083	0.11909	-0.03526	0.00344	0.84927	0.00282
		12.26	3.139	0.268	0.699	0.912477	0.190653	-0.05973	0.006296	0.810831	0.00151
		12.29	5.635	0.004	0.781	0.979884	0.194899	-0.03348	0.000617	0.851637	0.001944
		5.24	4.873	0.132	0.789	0.893925	0.21504	-0.054356	0.0045	0.852792	-0.010521
		5.2	2.429	0.155	0.577	0.953321	0.012197	0.016991	-0.003251	0.864399	-0.00156
		5.22	2.986	0.222	0.665	0.900151	0.125606	-0.026586	0.001828	0.87353	-0.005379
		5.22	3.455	0.246	0.715	0.956869	0.088393	-0.01627	0.001445	0.793899	0.00175
		5.24	5.403	0.018	0.784	0.925927	0.172571	-0.020712	-0.002073	0.877573	-0.006437
		7.92	4.832	0.167	0.79	0.939052	0.169982	-0.029653	0.000209	0.845159	-0.015785
		7.89	2.384	0.165	0.575	0.940629	0.094186	-0.02389	0.001851	0.865774	0.002047
		7.91	3.158	0.255	0.691	0.904107	0.153667	-0.041693	0.004094	0.813208	0.001219
		7.91	3.704	0.271	0.746	0.944834	0.086077	-0.00238	-0.001587	0.803175	-0.009312
		7.92	5.56	0.009	0.784	0.981626	0.124296	-0.006153	-0.002764	0.92707	-0.033614
A66	6	12.26	3.598	0.275	0.871	0.964485	0.23036	-0.060846	0.003977	0.764816	0.003473
		12.35	4.759	0.173	0.935	0.988915	0.299302	-0.050668	0.000761	0.716402	0.025911
		12.19	2.462	0.143	0.644	0.958536	0.097907	-0.030973	0.003985	0.868781	-0.012702
		12.22	2.945	0.219	0.748	0.931138	0.262248	-0.102677	0.012664	0.847851	-0.00939
		12.4	5.599	0.004	0.955	1.022912	0.32476	-0.064431	0.00458	0.709366	0.040797
		5.2	2.294	0.104	0.611	0.93802	0.06425	-0.013777	0.001319	0.836754	0.007409
		5.21	2.874	0.179	0.725	0.913328	0.188338	-0.053355	0.004549	0.790354	0.006919
		5.22	3.412	0.233	0.825	0.940419	0.223776	-0.061792	0.004934	0.811134	-0.008369
		5.25	4.512	0.173	0.924	0.951027	0.307873	-0.071552	0.005581	0.783509	-0.00525
		5.27	5.327	0.018	0.944	0.974793	0.382666	-0.110381	0.013859	0.723366	0.044927
		8.12	4.724	0.163	0.926	0.963916	0.355102	-0.103836	0.012358	0.714263	0.031462
		8.03	2.64	0.168	0.682	0.999248	0.034531	0.007534	-0.00266	0.817408	0.022235
		8.03	3.055	0.255	0.77	0.991762	0.145341	-0.047007	0.005203	0.806471	-0.004033
		8.04	3.658	0.261	0.864	0.969555	0.149501	-0.013813	-0.001765	0.739394	0.00154
		8.13	5.523	0.008	0.952	0.985111	0.383061	-0.111052	0.014025	0.733098	0.026906

Continued

	Blade						Tip vortex radius			Tip vortex pitch	
Config	pitch	Speed	TSR	Cp	CT	A	B	C	D	E	F
A88	8	12.29	3.479	0.285	0.799	0.948207	0.175851	-0.037318	0.001796	0.719571	0.024385
		12.35	4.703	0.21	0.875	0.980809	0.218434	-0.030718	-0.000369	0.745755	0.018843
		12.21	1.775	0.076	0.479	0.831569	0.130114	-0.046732	0.006065	0.690715	0.069578
		12.25	2.8	0.219	0.686	0.928522	0.195154	-0.052178	0.003208	0.854139	-0.000559
		12.38	5.68	0.004	0.872	0.961197	0.32551	-0.080796	0.00773	0.807227	0.004051
		5.16	2.415	0.137	0.608	0.835191	0.116898	-0.026378	0.002098	0.835206	0.015112
		5.18	3	0.216	0.715	0.896951	0.171396	-0.046347	0.004126	0.848375	-0.005641
		5.18	3.474	0.246	0.78	0.929805	0.096351	0.005488	-0.003897	0.795737	-0.004305
		5.21	4.606	0.18	0.864	0.941231	0.244817	-0.059794	0.00475	0.814379	-0.003972
		5.23	5.455	0.018	0.878	0.927769	0.312204	-0.077822	0.00685	0.748633	0.049106
		8.11	4.77	0.18	0.867	0.943426	0.237791	-0.035776	-0.000574	0.783796	0.002018
		8.02	2.195	0.118	0.562	0.990057	-0.054879	0.033112	-0.004503	0.861086	0.000539
		8.05	3.686	0.271	0.807	0.948638	0.093812	0.011351	-0.004852	0.741847	0.006341
		8.15	5.599	0.009	0.872	0.991092	0.226068	-0.036768	0.001935	0.781964	0.016848
Fixed p	fix	6.13	6.511	0.101	0.816	0.989976	0.236636	-0.093302	0.01169	0.625391	0.203684
		6.11	3.645	0.308	0.724	0.959764	0.115313	-0.030109	0.002893	0.815905	-0.002435
		6.13	5.665	0.215	0.802	1.000003	0.142583	-0.024016	0.000286	0.823041	0.012304
		6.12	6.965	0.007	0.813	0.98597	0.234774	-0.097826	0.013499	0.575655	0.298482
		8.01	3.853	0.33	0.746	0.965655	0.103485	-0.019351	0.001196	0.807054	-0.000146
		8.02	6.497	0.144	0.827	0.943141	0.332195	-0.150438	0.023256	0.825176	0.007342
		8.03	5.647	0.248	0.817	0.998666	0.102398	0.018913	-0.0084	0.865234	-0.022769
		7.99	7.183	0.004	0.824	0.926512	0.384033	-0.184729	0.029074	0.619605	0.199171
B77	7	8.09	3.799	0.24	0.653	0.960341	0.107347	-0.021339	0.001394	0.814898	0.00147
		8.09	4.662	0.269	0.732	0.994868	0.084964	0.001403	-0.002808	0.854875	-0.024422
		8.1	5.669	0.225	0.795	0.973819	0.224134	-0.068139	0.007254	0.794754	0.008454
		8.06	3.031	0.152	0.542	0.951784	0.091752	-0.025552	0.002571	0.875452	-5.98E-05
		8.13	7.218	0.011	0.845	0.962573	0.26875	-0.073514	0.007509	0.854975	-0.02003
A610	6 & 10	8.06	4.547	0.198	0.858	0.882786	0.39286	-0.144032	0.0167	0.816162	-0.023497
		7.99	2.187	0.117	0.56	0.885572	0.109736	-0.02132	0.001083	0.96548	-0.032798
		8	2.679	0.188	0.655	0.950522	0.084622	-0.01217	-0.00047	0.85766	-0.003239
		8.03	3.66	0.266	0.806	0.933806	0.169368	-0.034686	0.001358	0.793037	-0.009192
		8.08	5.469	0.008	0.859	0.994144	0.13812	0.011333	-0.006664	1.427355	-0.000669

A special remark on the behavior of the unsymmetric configuration is pertinent. Configuration 610 had different pitch for the two blades. The flow was characterized by the differing strength of the circulations, from the two blades, which was evident in the photographs as a tendency for the tip vortices to form pairs. Thus, the pitch of the vortices became very “zig-zaggy”. Surprizingly, however, the radial positions seemed smoother. The curve fit to the spiral pitch, in this case, then appears relatively less relevant than that of the the radius. The performance, in terms of Cp and CT, seems to be close to the performance of a symmetric rotor with a pitch in between 6 and 10, i.e. 8. If this observation can be extended to all cases is unknown.

Performance of the turbine with the blades reduced in chord is presented below together with the A rotor performance for comparison.

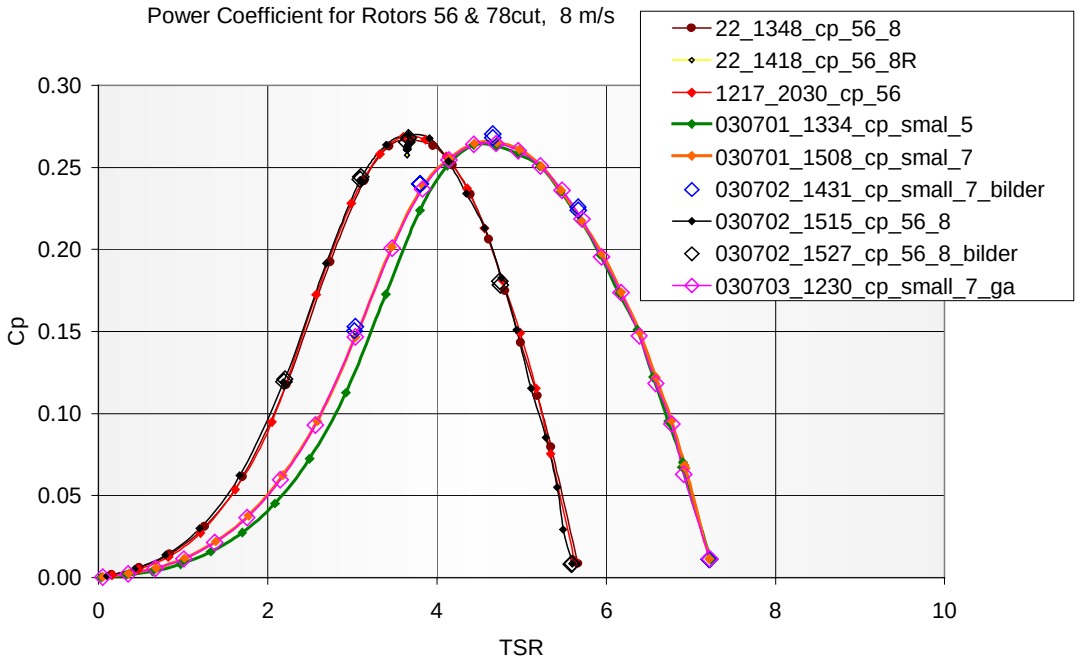

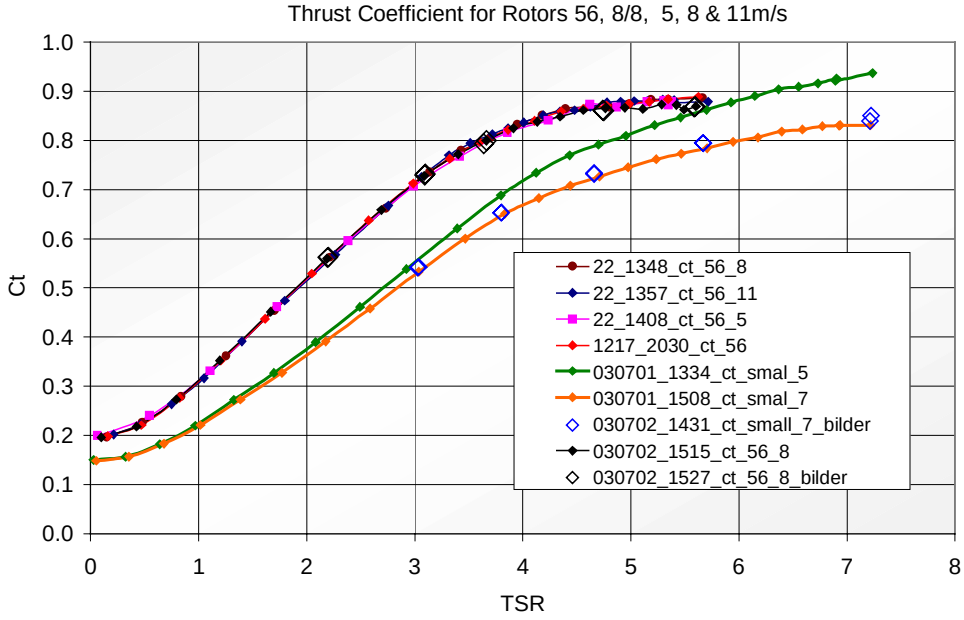

The performance chart seen below is plots directly from the data in the tables on the previous pages.
Because of the limitations of the laboratory setup and lack of time the TSR range is not adequately covered.

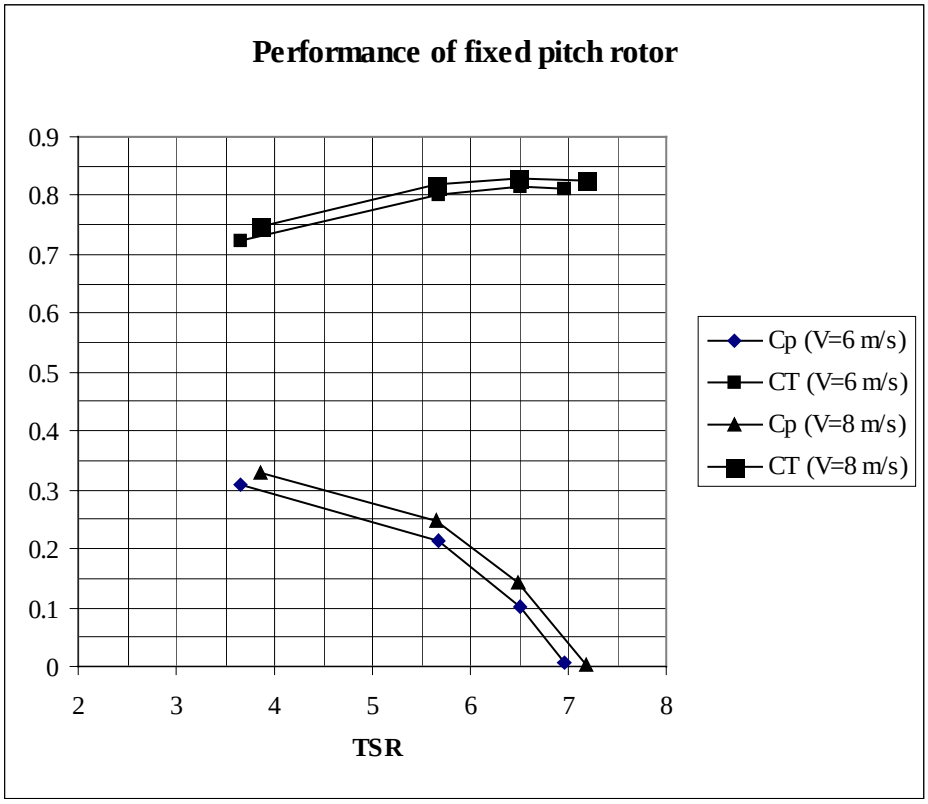

APPENDIX B – **Fix Pitch Rotor Geometry**

The geometry of the fix pitch rotor is presented as two photographs and curves showing the distribution of chord length and twist. Since the rotor was created with relatively primitive methods the two blades were sufficiently different to warrant separate descriptions. Thus, reference will be made to “blade 1” and “blade 2”. Blade sections 1 through 5 were cut out from blade 1, while sections 6 through 10 are from blade 2. In order to be able to evaluate the sectional geometries the following table is provided.

Blade 1

Profile section order number	Radial position r/R … where R = 125 mm
1	.95
2	.8
3	.6
4	.4
5	.29

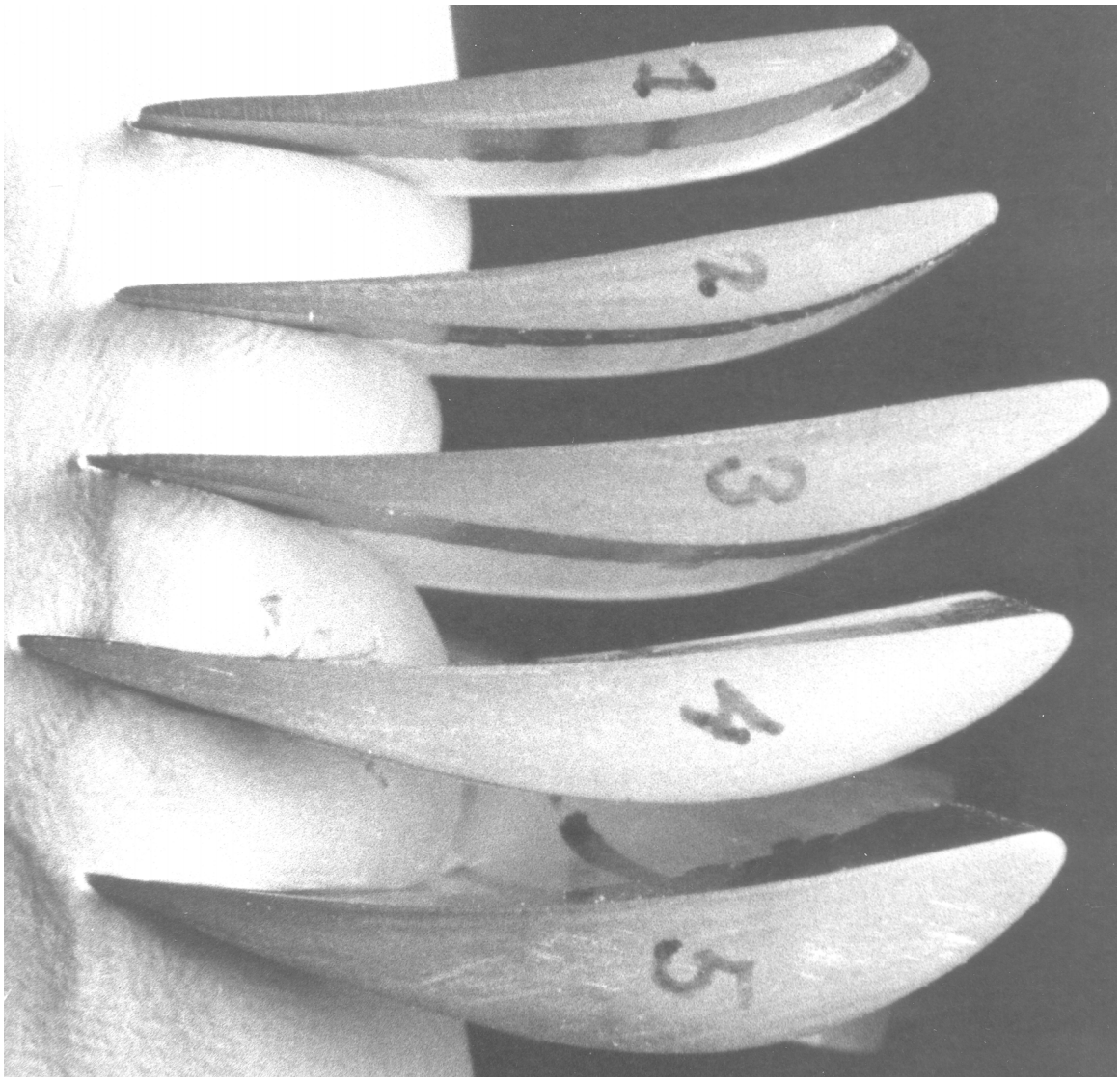

Blade 2

Profile section order number	Radial position r/R … where R = 125 mm
10	.95
9	.8
8	.6
7	.4
6	.29

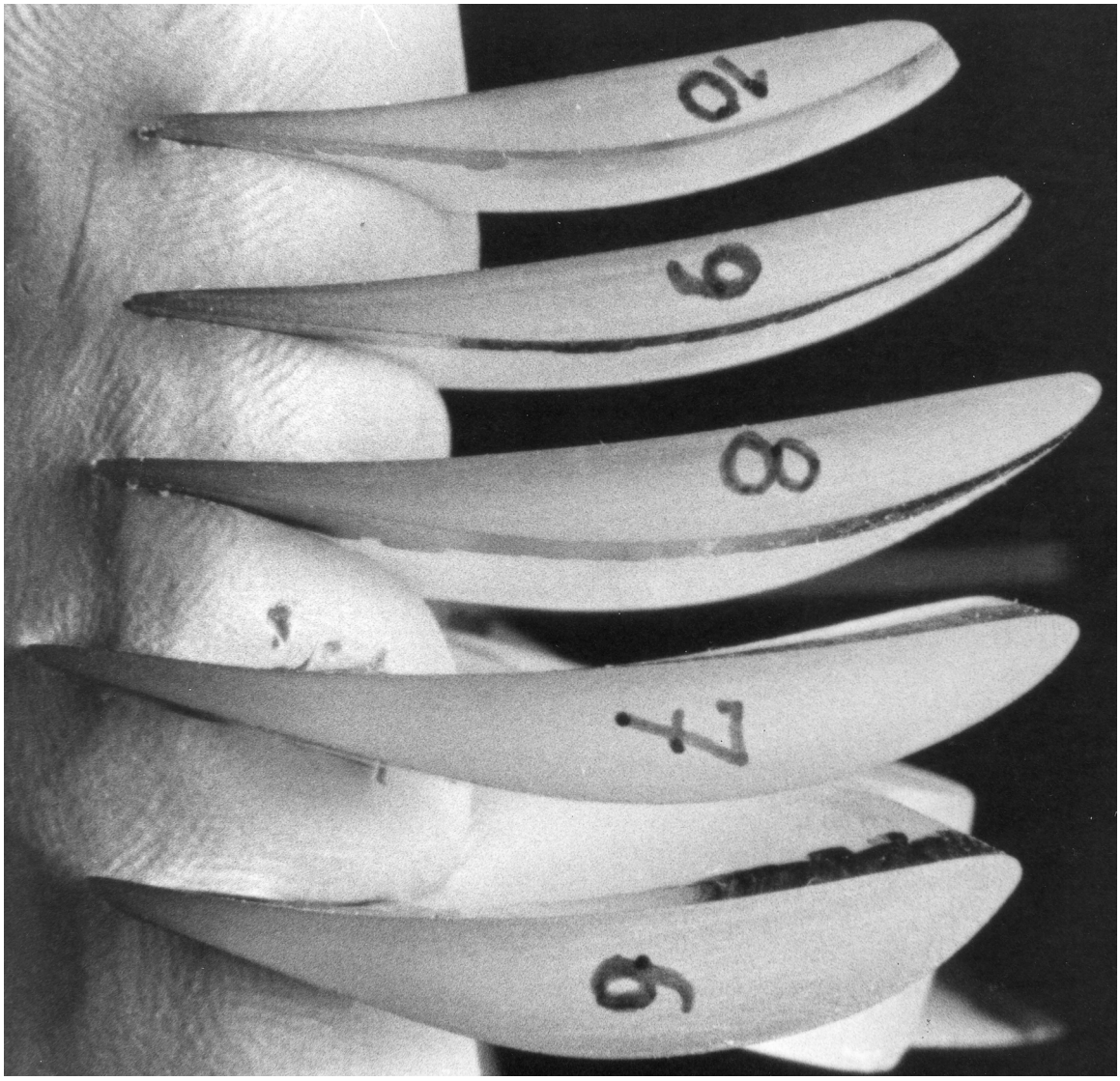

For proper interpretation it is necessary to know that the blades were of slightly different length.

Length of blade 1 = 122.5 mm; Length of blade 2 = 125 mm

The reference length R = 125 mm.

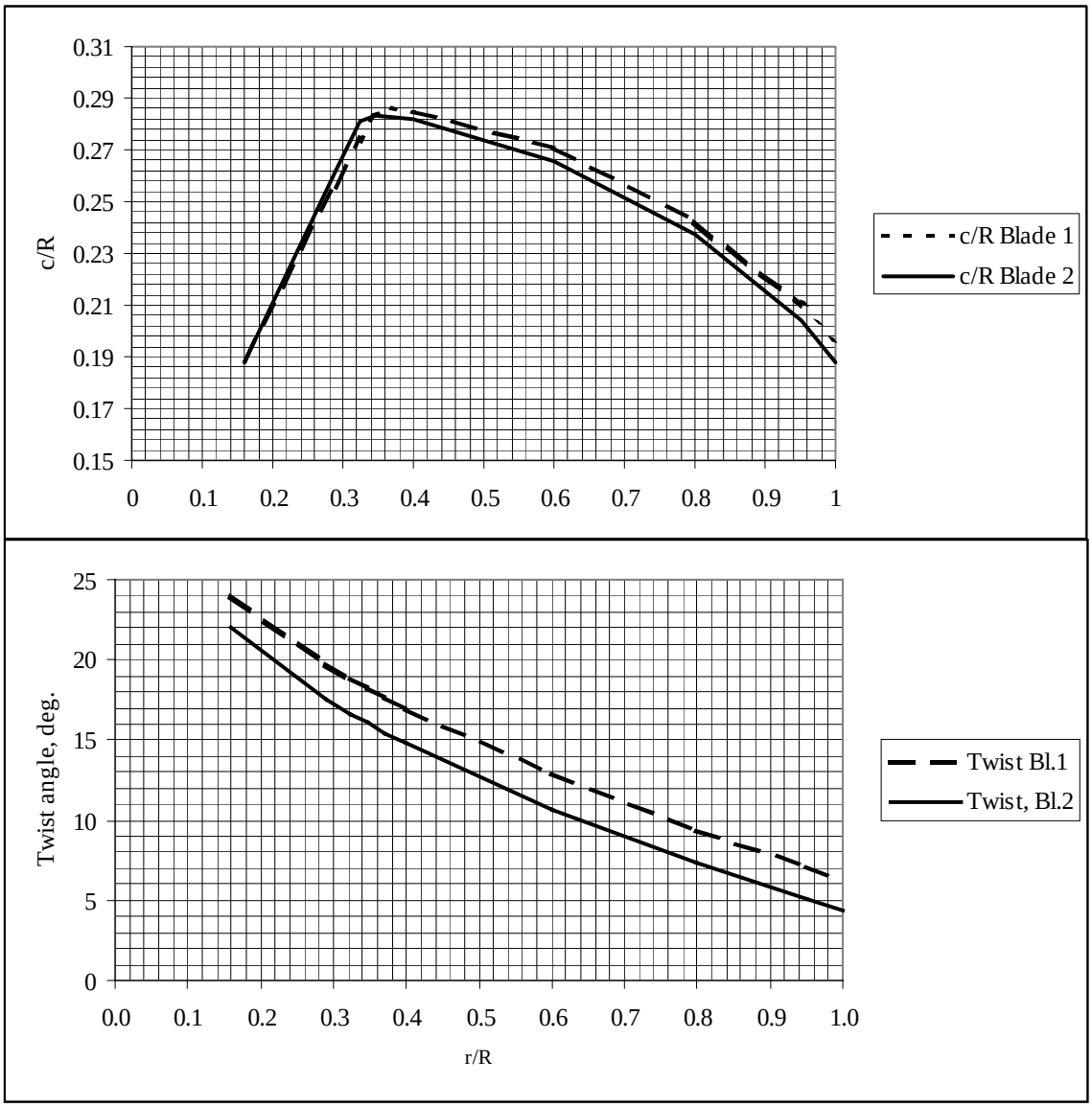

The section photographs can be analyzed such that the section coordinates can be evaluated. Having the section pictures on the computer screen in a program with window coordinates will make it much easier to evaluate the coordinates. It is the intent to maintain the files that contain the photographs for the interested reader to analyze in a suitable way. It is also imaginable that it would be of interest to generate the 2D aerodynamic tables, using e.g. XFOIL, for BEM calculations. XFOIL requires the section coordinates as input.